Journal of Solid Mechanics Vol. 11, No. 4 (2019) pp. 790-808
DOI: 10.22034/jsm.2019.668763

Efficient Higher-Order Shear Deformation Theories for Instability Analysis of Plates Carrying a Mass Moving on an Elliptical Path

E. Torkan [1], M. Pirmoradian [2,*]

[1]*Young Researchers and Elite Club, Khomeinishahr Branch, Islamic Azad University, Khomeinishahr, Isfahan,Iran*
[2]*Department of Mechanical Engineering, Khomeinishahr Branch, Islamic Azad University, Khomeinishahr, Isfahan, Iran*

Received 21 July 2019; accepted 21 September 2019

ABSTRACT

The dynamic performance of structures under traveling loads should be exactly analyzed to have a safe and reasonable structural design. Different higher-order shear deformation theories are proposed in this paper to analyze the dynamic stability of thick elastic plates carrying a moving mass. The displacement fields of different theories are chosen based upon variations along the thickness as cubic, sinusoidal, hyperbolic and exponential. The well-known Hamilton's principle is utilized to derive equations of motion and then they are solved using the Galerkin method. The energy-rate method is used as a numerical method to calculate the boundary curves separating the stable and unstable regions in the moving mass parameters plane. Effects of the relative plate thickness, trajectories radii and the Winkler foundation stiffness on the system stability are examined. The results obtained in this research are compared, in a special case, with those of the Kirchhoff's plate model for the validation.

Keywords: Mass–plate interaction; Higher-order shear deformation theories; Parametric vibration; Parametric resonance; Energy-rate method.

1 INTRODUCTION

VIBRATIONS occur in many structures and machines and can devastatingly affect the system performance. Thus, investigating the behavior of dynamic systems is vital to prevent unwanted vibrations and the resonance phenomenon. Plates are among the most important structures in the mechanical engineering applications that sometimes go under in plane, shear and moving forces. A lot of analytical and numerical studies conducted in the field of moving loads are related to one-dimensional structures like cables and beams [1, 2], which have simpler governing equations compared to plates [3, 4]. However, the dynamic analysis of plates under the influence of traveling loads has also been performed by some researchers [3, 5–9]. Although there are some papers regarding this issue, however most of them have been carried out on thin plates and based on the Kirchhoff's plate theory. In these studies, a group of

*Corresponding author.
E-mail address: pirmoradian@iaukhsh.ac.ir (M. Pirmoradian).

researchers analyzed the dynamic response of plates under moving loads by neglecting the inertial effects of the moving masses [3, 10]. In addition, nonlinear dynamic analyses of the plate-moving mass system [5, 6], investigation of inertial terms effects of moving masses on the system response [11], different assumptions on the mass movement patterns (single or multiple and constant velocity or accelerating motion) [9, 12–14] were examined. Since modeling the plates using the Kirchhoff's plate theory is valid only for a small range of plate thicknesses, shear theories have been proposed to study the dynamic behavior of moderately thick plates. Gbadeyan and Dada [15] used the first-order shear deformation theory to examine the elastodynamic response of a thick rectangular plate under moving mass. Although their results were limited to the derivation of time response diagrams for the aforementioned system, they showed the importance of the rotary inertia and the shear deformation effects. Amiri et al. [16] conducted a comprehensive research on the dynamic response of moderately thick rectangular plates influenced by a mass moving along different paths. They derived the governing dynamic equations based on the first-order shear deformation theory and solved them using the eigenfunction expansion method. Nowadays, according to economic considerations, it is necessary to decrease the weight of structures carrying moving objects. This subject has increased the probability of large amplitude vibrations in aforementioned systems and accordingly identification and finding rules to control the undesirable vibrations have become a necessitation. One of the most important aspects of this issue is determination of conditions which induce instability in the structures carrying moving masses, where there is the possibility of irreparable damages if these conditions are not prevented.

The dynamic instability of elastic structures subjected to traveling loads can be due to different types of resonances including internal [17], external [18] and parametric [19–22]. In comparison with external resonance which occurs because of a synchronization between external excitation frequency and the natural frequency of the system, the internal resonance can be due to nonlinear modes interference of a system at certain frequency ratios. The parametric resonance, on the other hand, is predicted to happen usually in self-excited systems when the driving frequency of excitation terms is almost a multiple of the system fundamental natural frequency. Parametric resonance creates instability in linear systems by transcending a critical drive verge which would not be even restricted by linear damping elements and would grow boundlessly. As an early study, Nelson and Conover [19] investigated the instability caused by parametric resonance in Euler-Bernoulli beams under passage of successive series of moving masses. In recent years, Pirmoradian et al. [20, 21] examined the occurrence of parametric and external resonances in Euler-Bernoulli and Timoshenko beams excited by sequential moving masses. They extracted the boundaries of unstable regions in the mass-velocity plane of moving masses based on the Floquet theory. Torkan et al. [23, 24] studied the conditions suitable for occurrence of parametric resonance in the transverse vibration of rectangular plates under the successive passage of moving masses. The plate was modeled based on the Kirchhoff's theory in the mentioned research and rectilinear and diagonal paths were considered for the sequence of masses. Pirmoradian et al. [25] studied the dynamic instability of thin rectangular plates with different boundary conditions under the traverse of moving masses by implementing the incremental harmonic balance method.

Three types of rectilinear, diagonal and circular paths were considered for the passage of the masses. What were reviewed in the above is a selection of some studies related to the parametric resonance conditions in the interaction between elastic structures and moving masses. Although instability analyses of beams under moving masses have been abundantly performed [19–21, 26], stability study of plate structures influenced by moving masses has been considered only in [23] and [25]. As mentioned earlier, the system modeling in the mentioned references was based on the Kirchhoff's theory, so there is a feasibility available for using the shear deformation theories. Accordingly, in this paper, the dynamic stability of a thick rectangular plate carrying a mass moving on an elliptical path is analyzed based upon the higher-order shear deformation theories.

2 MATHEMATICAL MODELING

There exist several different theories for describing the dynamic and static behaviors of elastic plates which are chosen based on the plates geometry and their constituent materials. Developing and studying plate theories started from mid-19th century and are still in progress. These theories can be divided into three categories including Kirchhoff's plate theory, the first-order shear deformation theory and the higher-order shear deformation theory. The Kirchhoff's plate theory which is the simplest one to express the plate behavior is based on the assumption that the vectors perpendicular to the mid-plane do not rotate, and do not experience any extension or deformation. Although this classic theory provides exact results for thin plates, because of neglecting the shear deformation it cannot yield exact results for thick plates. In the first-order shear deformation theory, more exact results will be obtained according to consideration of shear deformations in the governing equations. However, the drawback of this method is the need for

a suitable choice of correction shear factor which makes this theory slightly difficult to use. Therefore, researchers have developed the higher-order shear deformation theories. Some of the most famous ones are the third-order shear deformation theory (TSDT) [27], the improved third-order shear deformation theory (ITSDT) [28], the sinusoidal shear deformation theory (SSDT) [29], the exponential shear deformation theory (ESDT) [30] and the hyperbolic shear deformation theory (HSDT) [31].

The structure under study in this problem is a uniform rectangular plate with the length of *a*, width of *b*, constant thickness of *h*, Young's modulus of *E*, Poisson's ratio of *v*, mass per unit volume of ρ and with simply supported boundary conditions which is placed on an elastic Winkler's foundation with the stiffness of k_w (as Fig. 1).

The coordinate axes are chosen so that the $x-y$ plane is coincident with plate mid-plane and the *z* axis is perpendicular to it. Also, it is assumed that the moving mass *M* travels on an arbitrary path on the plate's surface.

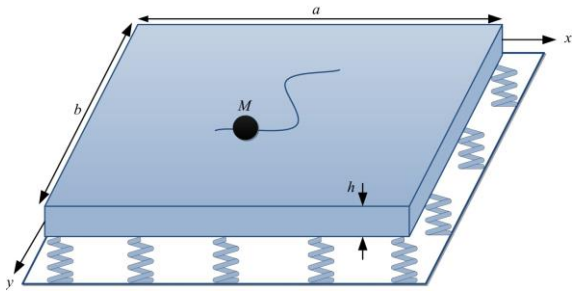

Fig.1
The schematic of the plate carrying a mass moving on an arbitrary path.

In order to invoke the Hamilton's principle, the displacement field relations based on the higher-order shear deformation theories are defined as the following:

$$\bar{u}(x,y,z)=u(x,y)-z\,w_{,x}+f(z)\left(\psi_x+w_{,x}\right), \tag{1}$$

$$\bar{v}(x,y,z)=v(x,y)-z\,w_{,y}+f(z)\left(\psi_y+w_{,y}\right), \tag{2}$$

$$\bar{w}(x,y,z)=w(x,y), \tag{3}$$

where u, v and w are the plate mid-plane displacements. In additions, ψ_x and ψ_y are shear deformations about *x* and *y* axes. The function $f(z)$ for different higher-order shear deformation theories is presented in Table 1.

Table 1
The expressions for $f(z)$ function for various shear theories.

Theory	$f(z)$
TSDT	$f(z)=z\left(1-\frac{4z^2}{3h^2}\right)$
ITSDT	$f(z)=\frac{5}{4}z\left(1-\frac{4z^2}{3h^2}\right)$
SSDT	$f(z)=\frac{h}{\pi}\sin\left(\pi\frac{z}{h}\right)$
ESDT	$f(z)=ze^{-2\left(\frac{z}{h}\right)^2}$
HSDT	$f(z)=\frac{z\cosh\left(\frac{\pi}{2}\right)-\frac{h}{\pi}\sinh\left(\pi\frac{z}{h}\right)}{\cosh\left(\frac{\pi}{2}\right)-1}$

Strains due to small deflections and based on the higher-order shear deformation theories are as the following:

$$\begin{Bmatrix} \varepsilon_{xx} \\ \varepsilon_{yy} \\ \gamma_{xy} \end{Bmatrix} = \begin{Bmatrix} \varepsilon_{xx}^{(0)} \\ \varepsilon_{yy}^{(0)} \\ \gamma_{xy}^{(0)} \end{Bmatrix} + z \begin{Bmatrix} \varepsilon_{xx}^{(1)} \\ \varepsilon_{yy}^{(1)} \\ \gamma_{xy}^{(1)} \end{Bmatrix} + z^3 \begin{Bmatrix} \varepsilon_{xx}^{(3)} \\ \varepsilon_{yy}^{(3)} \\ \gamma_{xy}^{(3)} \end{Bmatrix}, \tag{4}$$

$$\begin{Bmatrix} \gamma_{yz} \\ \gamma_{xz} \end{Bmatrix} = \begin{Bmatrix} \gamma_{yz}^{(0)} \\ \gamma_{xz}^{(0)} \end{Bmatrix} + z^2 \begin{Bmatrix} \gamma_{yz}^{(2)} \\ \gamma_{xz}^{(2)} \end{Bmatrix}. \tag{5}$$

In which ε_{xx} and ε_{yy} are normal strains and γ_{xy}, γ_{yz} and γ_{xz} are shear strains. Also, in recent expressions we have:

$$\begin{Bmatrix} \varepsilon_{xx}^{(0)} \\ \varepsilon_{yy}^{(0)} \\ \gamma_{xy}^{(0)} \end{Bmatrix} = \begin{Bmatrix} \dfrac{\partial u}{\partial x} \\ \dfrac{\partial v}{\partial y} \\ \dfrac{\partial u}{\partial y} + \dfrac{\partial v}{\partial x} \end{Bmatrix}, \quad \begin{Bmatrix} \varepsilon_{xx}^{(1)} \\ \varepsilon_{yy}^{(1)} \\ \gamma_{xy}^{(1)} \end{Bmatrix} = \begin{Bmatrix} \dfrac{\partial \psi_x}{\partial x} \\ \dfrac{\partial \psi_y}{\partial y} \\ \dfrac{\partial \psi_x}{\partial y} + \dfrac{\partial \psi_y}{\partial x} \end{Bmatrix}, \tag{6}$$

$$\begin{Bmatrix} \varepsilon_{xx}^{(3)} \\ \varepsilon_{yy}^{(3)} \\ \gamma_{xy}^{(3)} \end{Bmatrix} = -c_1 \begin{Bmatrix} \left(\dfrac{\partial \psi_x}{\partial x} + \dfrac{\partial^2 w}{\partial x^2} \right) \\ \left(\dfrac{\partial \psi_y}{\partial y} + \dfrac{\partial^2 w}{\partial y^2} \right) \\ \left(\dfrac{\partial \psi_x}{\partial y} + \dfrac{\partial \psi_y}{\partial x} + 2\dfrac{\partial^2 w}{\partial x \partial y} \right) \end{Bmatrix}, \tag{7}$$

$$\begin{Bmatrix} \gamma_{yz}^{(0)} \\ \gamma_{xz}^{(0)} \end{Bmatrix} = c_2 \begin{Bmatrix} \psi_y + \dfrac{\partial w}{\partial y} \\ \psi_x + \dfrac{\partial w}{\partial x} \end{Bmatrix}, \quad \begin{Bmatrix} \gamma_{yz}^{(2)} \\ \gamma_{xz}^{(2)} \end{Bmatrix} = -c_3 \begin{Bmatrix} \psi_y + \dfrac{\partial w}{\partial y} \\ \psi_x + \dfrac{\partial w}{\partial x} \end{Bmatrix}. \tag{8}$$

The coefficients of c_1, c_2 and c_3 are determined based on different theories. For example, these coefficients for TSDT and ITSDT are [32]:

$$c_1 = \frac{4}{3h^2}, \qquad c_2 = 1, \qquad c_3 = \frac{4}{h^2}, \quad \text{for TSDT} \tag{9}$$

$$c_1 = \frac{5}{3h^2} - \frac{1}{4z^2}, \quad c_2 = \frac{5}{4}, \quad c_3 = \frac{5}{h^2}, \quad \text{for ITSDT} \tag{10}$$

By considering the linear elastic behavior, the normal stresses $\left(\sigma_{xx}, \sigma_{yy}\right)$ and shear stresses $\left(\tau_{xy}, \tau_{yz}, \tau_{xz}\right)$ can be represented in the matrix form as follows:

$$\begin{Bmatrix}\sigma_{xx}\\ \sigma_{yy}\\ \tau_{xz}\\ \tau_{yz}\\ \tau_{xy}\end{Bmatrix}=\begin{bmatrix}Q_{11} & Q_{12} & 0 & 0 & 0\\ Q_{12} & Q_{22} & 0 & 0 & 0\\ 0 & 0 & Q_{44} & 0 & 0\\ 0 & 0 & 0 & Q_{55} & 0\\ 0 & 0 & 0 & 0 & Q_{66}\end{bmatrix}\begin{Bmatrix}\varepsilon_{xx}\\ \varepsilon_{yy}\\ \gamma_{xz}\\ \gamma_{yz}\\ \gamma_{xy}\end{Bmatrix}. \tag{11}$$

It should be noted that similar to the classic and the first-order shear deformation theories, the normal transverse stress (σ_{zz}) is assumed to be zero. The coefficients Q_{ij} appearing in Eq. (11) are related to engineering constants and they are as follows:

$$Q_{11}=Q_{22}=\frac{E}{1-\nu^2},\qquad Q_{12}=\frac{\nu E}{1-\nu^2},\qquad Q_{44}=Q_{55}=Q_{66}=G=\frac{E}{2(1+\nu)}. \tag{12}$$

The governing differential equations of motion are derived using the Hamilton's principle which is given as:

$$\int_0^t(\delta U+\delta V-\delta K)dt=0, \tag{13}$$

where U is the strain energy of the plate, V is the work done by the applied forces and K is the kinetic energy of the plate which are going to be derived in the following. The variational form of the virtual strain energy function for an elastic plate is as follows:

$$\delta U=\int_A\int_{-h/2}^{h/2}\left[\sigma_{xx}\,\delta\varepsilon_{xx}+\sigma_{yy}\,\delta\varepsilon_{yy}+\tau_{xy}\,\delta\gamma_{xy}+\tau_{xz}\,\delta\gamma_{xz}+\tau_{yz}\,\delta\gamma_{yz}\right]dz\,dA, \tag{14}$$

By substituting Eqs. (4) and (5) into Eq. (14), it yields:

$$\begin{aligned}\delta U=\int_A\int_{-h/2}^{h/2}\Big[&\sigma_{xx}\left(\delta\varepsilon_{xx}^{(0)}+z\,\delta\varepsilon_{xx}^{(1)}-c_1z^3\delta\varepsilon_{xx}^{(3)}\right)+\sigma_{yy}\left(\delta\varepsilon_{yy}^{(0)}+z\,\delta\varepsilon_{yy}^{(1)}-c_1z^3\delta\varepsilon_{yy}^{(3)}\right)\\&+\tau_{xy}\left(\delta\gamma_{xy}^{(0)}+z\,\delta\gamma_{xy}^{(1)}-c_1z^3\delta\gamma_{xy}^{(3)}\right)+\tau_{xz}\left(\delta\gamma_{xz}^{(0)}+z^2\delta\gamma_{xz}^{(2)}\right)+\tau_{yz}\left(\delta\gamma_{yz}^{(0)}+z^2\delta\gamma_{yz}^{(2)}\right)\Big]dz\,dA.\end{aligned} \tag{15}$$

The virtual work done on the system is defined as:

$$\delta V=-\int_A\left[\left(f_t(x,y,t)-k_ww\right)\delta w\right]dA, \tag{16}$$

where $f_t(x,y,t)$ is the transverse loading function and will be substituted along with the moving mass loading function. The virtual kinetic energy of the plate based on the higher-order shear deformation theories can be expressed as:

$$\begin{aligned}\delta K=\int_A\int_{-h/2}^{h/2}\rho\left(\dot{\bar{u}}\,\delta\dot{\bar{u}}+\dot{\bar{v}}\,\delta\dot{\bar{v}}+\dot{\bar{w}}\,\delta\dot{\bar{w}}\right)dz\,dA=\int_A\int_{-h/2}^{h/2}\rho\Bigg[&\left(\dot u+z\,\dot\psi_x-c_1z^3\frac{\partial\dot w}{\partial x}\right)\left(\delta\dot u+z\,\delta\dot\psi_x-c_1z^3\frac{\partial\delta\dot w}{\partial x}\right)\\&+\left(\dot v+z\,\dot\psi_y-c_1z^3\frac{\partial\dot w}{\partial y}\right)\left(\delta\dot v+z\,\delta\dot\psi_y-c_1z^3\frac{\partial\delta\dot w}{\partial y}\right)+\dot w\,\delta\dot w\Bigg]dz\,dA\\=\int_A\Bigg\{&I_0\dot u\,\delta\dot u+I_0\dot v\,\delta\dot v+\left[I_2\dot\psi_x-c_1I_4\left(\dot\psi_x+\frac{\partial\dot w}{\partial x}\right)\right]\delta\dot\psi_x\end{aligned} \tag{17}$$

$$-c_1\left[I_4\dot{\psi}_x - c_1 I_6\left(\dot{\psi}_x + \frac{\partial \dot{w}}{\partial x}\right)\right]\left(\delta\dot{\psi}_x + \frac{\partial \delta\dot{w}}{\partial x}\right) + \left[I_2\dot{\psi}_y - c_1 I_4\left(\dot{\psi}_y + \frac{\partial \dot{w}}{\partial y}\right)\right]\delta\dot{\psi}_y - c_1\left[I_4\dot{\psi}_y - c_1 I_6\left(\dot{\psi}_y + \frac{\partial \dot{w}}{\partial y}\right)\right]\left(\delta\dot{\psi}_y + \frac{\partial \delta\dot{w}}{\partial y}\right)\Bigg\} dA, \tag{17}$$

where I_i $(i = 0,2,4,6)$ are the inertial terms of the plate. These terms are defined as:

$$I_i = \int_{-h/2}^{h/2} \rho(z)^i \, dz, \quad (i = 0,2,4,6). \tag{18}$$

Substituting Eqs. (15-17) into Eq. (13) and performing some algebraic operations and mathematical simplifications, the coupled partial differential equations governing the lateral displacement of the system will be obtained as:

$$\begin{aligned} &S_3Gh\left(\frac{\partial \psi_x}{\partial x} - \frac{\partial^2 w}{\partial x^2}\right) + S_3Gh\left(\frac{\partial \psi_y}{\partial y} - \frac{\partial^2 w}{\partial y^2}\right) - D\left[(S_1 - S_2)\left(\frac{\partial^3 \psi_x}{\partial x^3} + \nu\frac{\partial^3 \psi_y}{\partial x^2 \partial y}\right)\right. \\ &\left. - S_1\left(\frac{\partial^4 w}{\partial x^4} + \nu\frac{\partial^4 w}{\partial x^2 \partial y^2}\right)\right] - D\left[(S_1 - S_2)\left(\frac{\partial^3 \psi_y}{\partial y^3} + \nu\frac{\partial^3 \psi_x}{\partial x \partial y^2}\right) - S_1\left(\frac{\partial^4 w}{\partial y^4} + \nu\frac{\partial^4 w}{\partial x^2 \partial y^2}\right)\right] \\ &- \frac{D(1-\nu)}{2}\left[2(S_1 - S_2)\left(\frac{\partial^3 \psi_x}{\partial x \partial y^2} + \frac{\partial^3 \psi_y}{\partial x^2 \partial y}\right) - 4S_1\frac{\partial^4 w}{\partial x^2 \partial y^2}\right] + k_w w + \rho h\frac{\partial^2 w}{\partial t^2} \\ &- S_1\rho J\left(\frac{\partial^4 w}{\partial x^2 \partial t^2} + \frac{\partial^4 w}{\partial y^2 \partial t^2}\right) - (S_1 - S_2)\rho J\left(\frac{\partial^3 \psi_x}{\partial x \partial t^2} + \frac{\partial^3 \psi_y}{\partial y \partial t^2}\right) = f_t(x, y, t), \end{aligned} \tag{19}$$

$$\begin{aligned} &-D\left[(1 + S_1 - 2S_2)\left(\frac{\partial^2 \psi_x}{\partial x^2} + \nu\frac{\partial^2 \psi_y}{\partial x \partial y}\right) - (S_1 - S_2)\left(\frac{\partial^3 w}{\partial x^3} + \nu\frac{\partial^3 w}{\partial x \partial y^2}\right)\right] \\ &- \frac{D(1-\nu)}{2}\left[(1 + S_1 - 2S_2)\left(\frac{\partial^2 \psi_x}{\partial y^2} + \frac{\partial^2 \psi_y}{\partial x \partial y}\right) - 2(S_1 - S_2)\left(\frac{\partial^3 w}{\partial x \partial y^2}\right)\right] \\ &+ S_3Gh\left(\psi_x - \frac{\partial w}{\partial x}\right) + (1 + S_1 - 2S_2)\rho J\frac{\partial^2 \psi_x}{\partial t^2} + (S_1 - S_2)\rho J\left(\frac{\partial^3 w}{\partial x \partial t^2}\right) = 0, \end{aligned} \tag{20}$$

$$\begin{aligned} &-D\left[(1 + S_1 - 2S_2)\left(\frac{\partial^2 \psi_y}{\partial y^2} + \nu\frac{\partial^2 \psi_x}{\partial x \partial y}\right) - (S_1 - S_2)\left(\frac{\partial^3 w}{\partial y^3} + \nu\frac{\partial^3 w}{\partial x^2 \partial y}\right)\right] \\ &- \frac{D(1-\nu)}{2}\left[(1 + S_1 - 2S_2)\left(\frac{\partial^2 \psi_y}{\partial x^2} + \frac{\partial^2 \psi_x}{\partial x \partial y}\right) - 2(S_1 - S_2)\left(\frac{\partial^3 w}{\partial x^2 \partial y}\right)\right] \\ &+ S_3Gh\left(\psi_y - \frac{\partial w}{\partial y}\right) + (1 + S_1 - 2S_2)\rho J\frac{\partial^2 \psi_y}{\partial t^2} + (S_1 - S_2)\rho J\left(\frac{\partial^3 w}{\partial y \partial t^2}\right) = 0, \end{aligned} \tag{21}$$

where the coefficients S_1, S_2 and S_3 are presented in Table 2 based on different higher-order shear deformation theories.

Table 2
Values of S_1, S_2 and S_3 based on various shear deformation theories.

Theory	S_1	S_2	S_3
TSDT	$\frac{1}{21}$	$\frac{1}{5}$	$\frac{8}{15}$
ITSDT	$\frac{1}{84}$	0	$\frac{5}{6}$
SSDT	$\frac{5873}{98123}\approx 0.0559$	$\frac{35208}{155813}\approx 0.226$	$\frac{1}{2}$
ESDT	$\frac{9474}{128279}\approx 0.0739$	$\frac{25283}{100044}\approx 0.253$	$\frac{16822}{35935}\approx 0.468$
HSDT	$\frac{12007}{311296}\approx 0.0386$	$\frac{5380}{30127}\approx 0.179$	$\frac{21999}{39088}\approx 0.536$

The external excitation force caused by the mass movements on an arbitrary path is defined as:

$$f_t\left(x,y,t\right)=M\left(g-\frac{d^2w}{dt^2}\right)\bar{\delta}\left(x-x_M\left(t\right)\right)\bar{\delta}\left(y-y_M\left(t\right)\right), \tag{22}$$

where g introduces the gravitational acceleration and $\bar{\delta}$ is the Dirac-delta function. Also, $x_M\left(t\right)$ and $y_M\left(t\right)$ introduce the mass location on the plate's surface at the time t. Assuming complete contact between the mass and the plate and considering all inertial terms, the loading function extends to:

$$\begin{aligned} f_t\left(x,y,t\right)=-M\Bigg(&-g+\frac{\partial^2w}{\partial t^2}+\frac{\partial^2w}{\partial x^2}\left(\frac{dx}{dt}\right)^2+\frac{\partial^2w}{\partial y^2}\left(\frac{dy}{dt}\right)^2+2\frac{\partial^2w}{\partial x\,\partial y}\left(\frac{dx}{dt}\right)\left(\frac{dy}{dt}\right)+2\frac{\partial^2w}{\partial x\,\partial t}\left(\frac{dx}{dt}\right)\\ &+2\frac{\partial^2w}{\partial y\,\partial t}\left(\frac{dy}{dt}\right)+\frac{\partial w}{\partial x}\left(\frac{d^2x}{dt^2}\right)+\frac{\partial w}{\partial y}\left(\frac{d^2y}{dt^2}\right)\Bigg)\bar{\delta}\left(x-x_M\left(t\right)\right)\bar{\delta}\left(y-y_M\left(t\right)\right). \end{aligned} \tag{23}$$

Finally by substituting Eq. (23) into Eq. (19), the partial differential equations governing the plate-moving mass system are obtained as:

$$\begin{aligned} &S_3Gh\left(\frac{\partial\psi_x}{\partial x}-\frac{\partial^2w}{\partial x^2}\right)+S_3Gh\left(\frac{\partial\psi_y}{\partial y}-\frac{\partial^2w}{\partial y^2}\right)-D\Bigg[\left(S_1-S_2\right)\left(\frac{\partial^3\psi_x}{\partial x^3}+\nu\frac{\partial^3\psi_y}{\partial x^2\partial y}\right)\\ &-S_1\left(\frac{\partial^4w}{\partial x^4}+\nu\frac{\partial^4w}{\partial x^2\partial y^2}\right)\Bigg]-D\Bigg[\left(S_1-S_2\right)\left(\frac{\partial^3\psi_y}{\partial y^3}+\nu\frac{\partial^3\psi_x}{\partial x\,\partial y^2}\right)-S_1\left(\frac{\partial^4w}{\partial y^4}+\nu\frac{\partial^4w}{\partial x^2\partial y^2}\right)\Bigg]\\ &-\frac{D\left(1-\nu\right)}{2}\Bigg[2\left(S_1-S_2\right)\left(\frac{\partial^3\psi_x}{\partial x\,\partial y^2}+\frac{\partial^3\psi_y}{\partial x^2\partial y}\right)-4S_1\frac{\partial^4w}{\partial x^2\partial y^2}\Bigg]+k_ww+\rho h\frac{\partial^2w}{\partial t^2}\\ &-S_1\rho J\left(\frac{\partial^4w}{\partial x^2\partial t^2}+\frac{\partial^4w}{\partial y^2\partial t^2}\right)-\left(S_1-S_2\right)\rho J\left(\frac{\partial^3\psi_x}{\partial x\,\partial t^2}+\frac{\partial^3\psi_y}{\partial y\,\partial t^2}\right)=-M\Bigg(-g+\frac{\partial^2w}{\partial t^2}\\ &+\frac{\partial^2w}{\partial x^2}\left(\frac{dx}{dt}\right)^2+\frac{\partial^2w}{\partial y^2}\left(\frac{dy}{dt}\right)^2+2\frac{\partial^2w}{\partial x\,\partial y}\left(\frac{dx}{dt}\right)\left(\frac{dy}{dt}\right)+2\frac{\partial^2w}{\partial x\,\partial t}\left(\frac{dx}{dt}\right)+2\frac{\partial^2w}{\partial y\,\partial t}\left(\frac{dy}{dt}\right)\\ &+\frac{\partial w}{\partial x}\left(\frac{d^2x}{dt^2}\right)+\frac{\partial w}{\partial y}\left(\frac{d^2y}{dt^2}\right)\Bigg)\bar{\delta}\left(x-x_M\left(t\right)\right)\bar{\delta}\left(y-y_M\left(t\right)\right), \end{aligned} \tag{24}$$

$$-D\left[\left(1+S_1-2S_2\right)\left(\frac{\partial^2\psi_x}{\partial x^2}+\nu\frac{\partial^2\psi_y}{\partial x\,\partial y}\right)-\left(S_1-S_2\right)\left(\frac{\partial^3 w}{\partial x^3}+\nu\frac{\partial^3 w}{\partial x\,\partial y^2}\right)\right]$$
$$-\frac{D\left(1-\nu\right)}{2}\left[\left(1+S_1-2S_2\right)\left(\frac{\partial^2\psi_x}{\partial y^2}+\frac{\partial^2\psi_y}{\partial x\,\partial y}\right)-2\left(S_1-S_2\right)\left(\frac{\partial^3 w}{\partial x\,\partial y^2}\right)\right] \tag{25}$$
$$+S_3Gh\left(\psi_x-\frac{\partial w}{\partial x}\right)+\left(1+S_1-2S_2\right)\rho J\frac{\partial^2\psi_x}{\partial t^2}+\left(S_1-S_2\right)\rho J\left(\frac{\partial^3 w}{\partial x\,\partial t^2}\right)=0,$$

$$-D\left[\left(1+S_1-2S_2\right)\left(\frac{\partial^2\psi_y}{\partial y^2}+\nu\frac{\partial^2\psi_x}{\partial x\,\partial y}\right)-\left(S_1-S_2\right)\left(\frac{\partial^3 w}{\partial y^3}+\nu\frac{\partial^3 w}{\partial x^2\partial y}\right)\right]$$
$$-\frac{D\left(1-\nu\right)}{2}\left[\left(1+S_1-2S_2\right)\left(\frac{\partial^2\psi_y}{\partial x^2}+\frac{\partial^2\psi_x}{\partial x\,\partial y}\right)-2\left(S_1-S_2\right)\left(\frac{\partial^3 w}{\partial x^2\partial y}\right)\right] \tag{26}$$
$$+S_3Gh\left(\psi_y-\frac{\partial w}{\partial y}\right)+\left(1+S_1-2S_2\right)\rho J\frac{\partial^2\psi_y}{\partial t^2}+\left(S_1-S_2\right)\rho J\left(\frac{\partial^3 w}{\partial y\,\partial t^2}\right)=0.$$

3 GALERKIN METHOD

After deriving the partial differential equations of motion, they are reduced to ordinary differential equations using the Galerkin method as a discretization method. For this purpose, first, the variables w, ψ_x and ψ_y are presented as a series of base functions according to the following expressions:

$$w\left(x,y,t\right)=\sum_{i=1}^{\infty}\tilde{w}_i\left(x,y\right)\bar{W}_i\left(t\right), \tag{27}$$

$$\psi_x\left(x,y,t\right)=\sum_{i=1}^{\infty}\tilde{\psi}_{xi}\left(x,y\right)\bar{\Psi}_{xi}\left(t\right), \tag{28}$$

$$\psi_y\left(x,y,t\right)=\sum_{i=1}^{\infty}\tilde{\psi}_{yi}\left(x,y\right)\bar{\Psi}_{yi}\left(t\right), \tag{29}$$

where $\bar{W}_i\left(t\right)$, $\bar{\Psi}_{xi}\left(t\right)$ and $\bar{\Psi}_{yi}\left(t\right)$ are time-dependent generalized coordinates and $\tilde{w}_i\left(x,y\right)$, $\tilde{\psi}_{xi}\left(x,y\right)$ and $\tilde{\psi}_{yi}\left(x,y\right)$ are the shape functions which have to be chosen appropriately to satisfy the boundary conditions. For a plate with simply supported boundary conditions, these shape functions are defined as:

$$\tilde{w}_i\left(x,y\right)=\sin\left(\frac{m\pi x}{a}\right)\sin\left(\frac{n\pi y}{b}\right), \tag{30}$$

$$\tilde{\psi}_{xi}\left(x,y\right)=\cos\left(\frac{m\pi x}{a}\right)\sin\left(\frac{n\pi y}{b}\right), \tag{31}$$

$$\tilde{\psi}_{yi}\left(x,y\right)=\sin\left(\frac{m\pi x}{a}\right)\cos\left(\frac{n\pi y}{b}\right), \tag{32}$$

where *m* and *n* are the vibration modes in the direction of plate length and width, respectively. Substituting Eqs. (27-29) into Eqs. (24-26), and then multiplying both sides of the obtained equations by $w_j(x,y)$, $\psi_{xj}(x,y)$ and $\psi_{yj}(x,y)$, respectively, and finally integrating the resulted equations over the plate's surface, the governing ordinary differential equations of the system are achieved in the form of vector-matrix as following:

$$M(t)\ddot{\bar{W}} + C(t)\dot{\bar{W}} + K(t)\bar{W} + D\ddot{\bar{\Psi}}_x + R\bar{\Psi}_x + B\ddot{\bar{\Psi}}_y + T\bar{\Psi}_y = F, \tag{33}$$

$$\bar{M}\ddot{\bar{W}} + \bar{D}\ddot{\bar{\Psi}}_x + \bar{R}\bar{\Psi}_x + \bar{K}\bar{W} + \bar{T}\bar{\Psi}_y = 0, \tag{34}$$

$$\tilde{M}\ddot{\bar{W}} + \tilde{B}\ddot{\bar{\Psi}}_y + \tilde{R}\bar{\Psi}_x + \tilde{K}\bar{W} + \tilde{T}\bar{\Psi}_y = 0, \tag{35}$$

where the vectors and matrices components are presented in Appendix A. Considering an elliptical path about the plate's center for the motion of the mass, the plate will be under an intermittent loading. Therefore, a parametric excitation would be imposed on the plate and consequently the governing equations would have periodic coefficients with respect to time. Rotary machineries and circular saws which are usually used in wood industries are some common industrial applications of this loading pattern. As shown in Fig. 2, it is assumed that the mass is moving about the plate center with angular velocity of ω on an elliptical path with semi-minor axis of a_0 and semi-major axis of b_0.

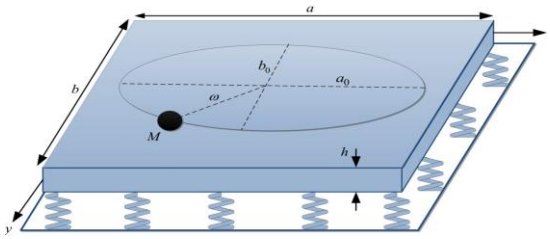

Fig.2
The schematic of the plate carrying a mass moving on an elliptical path.

Thus, the time-varying location of the mass on the plate is described by:

$$x_M(t) = x_0 - a_0\cos(\omega t), \tag{36}$$

$$y_M(t) = y_0 + b_0\sin(\omega t). \tag{37}$$

Substituting Eqs. (36) and (37) into Eqs. (33-35) and considering the first vibrational mode, the coupled time-varying ordinary differential equations of motion are obtained as:

$$\begin{aligned}
&\left[\frac{\rho hab}{4} + \frac{S_1}{4}\rho J\pi^2\left(\frac{a^2+b^2}{ab}\right) + MP_1(t)\right]\ddot{\bar{W}} + \left[2\frac{M\pi r}{a}\omega\sin(\omega t)P_2(t) - 2\frac{M\pi r}{b}\omega\cos(\omega t)P_3(t)\right]\dot{\bar{W}} \\
&+\left[\frac{S_3}{4}Gh\pi^2\left(\frac{a^2+b^2}{ab}\right) + \frac{S_1}{4}D\frac{\pi^4 b}{a^3}\left(\frac{a^4+b^4}{a^3b^3}\right) + \frac{S_1}{2}\nu D\frac{\pi^4}{ab} + \frac{S_1}{2}D(1-\nu)\frac{\pi^4}{ab} + k_w\frac{ab}{4} - \frac{M\pi^2r^2}{a^2}\omega^2\sin^2(\omega t)P_1(t)\right. \\
&-\frac{M\pi^2r^2}{b^2}\omega^2\cos^2(\omega t)P_1(t) - 2\frac{M\pi^2r^2}{ab}\omega^2\sin(\omega t)\cos(\omega t)P_4(t)P_5(t) + \frac{M\pi r}{a}\omega^2\cos(\omega t)P_2(t) \\
&\left.+\frac{M\pi r}{b}\omega^2\sin(\omega t)P_3(t)\right]\bar{W} + \left(\frac{S_1-S_2}{4}\right)\rho J\pi b\ddot{\bar{\Psi}}_x - \left[\frac{S_3}{4}Gh\pi b + \left(\frac{S_1-S_2}{4}\right)D\frac{\pi^3 b}{a^2} + \left(\frac{S_1-S_2}{4}\right)\nu D\frac{\pi^3}{b}\right. \\
&\left.+\left(\frac{S_1-S_2}{4}\right)D(1-\nu)\frac{\pi^3}{b}\right]\bar{\Psi}_x + \left(\frac{S_1-S_2}{4}\right)\rho J\pi a\ddot{\bar{\Psi}}_y - \left[\frac{S_3}{4}Gh\pi a + \left(\frac{S_1-S_2}{4}\right)\nu D\frac{\pi^3}{a} + \left(\frac{S_1-S_2}{4}\right)D\frac{\pi^3 a}{b^2}\right. \\
&\left.+\left(\frac{S_1-S_2}{4}\right)D(1-\nu)\frac{\pi^3}{a}\right]\bar{\Psi}_y = Mg\,P_5(t),
\end{aligned} \tag{38}$$

$$\left(\frac{S_1-S_2}{4}\right)\rho J\pi b\ddot{\bar{W}}+\left(\frac{1+S_1-2S_2}{4}\right)\rho Jab\ddot{\bar{\Psi}}_x+\left[\frac{S_3}{4}Ghab+\left(\frac{1+S_1-2S_2}{4}\right)D\frac{\pi^2 b}{a}+\left(\frac{1+S_1-2S_2}{8}\right)D(1-\nu)\frac{\pi^2 a}{b}\right]\bar{\Psi}_x$$
$$+\left[\left(\frac{1+S_1-2S_2}{4}\right)\nu D\pi^2+\left(\frac{1+S_1-2S_2}{8}\right)D(1-\nu)\pi^2\right]\bar{\Psi}_y-\left[\frac{S_3}{4}Gh\pi b+\left(\frac{S_1-S_2}{4}\right)D\frac{\pi^3 b}{a^2}+\left(\frac{S_1-S_2}{4}\right)\nu D\frac{\pi^3}{b}\right. \quad (39)$$
$$\left.+\left(\frac{S_1-S_2}{4}\right)D(1-\nu)\frac{\pi^3}{b}\right]\bar{W}=0,$$

$$\left(\frac{S_1-S_2}{4}\right)\rho J\pi a\ddot{\bar{W}}+\left(\frac{1+S_1-2S_2}{4}\right)\rho Jab\ddot{\bar{\Psi}}_y+\left[\left(\frac{1+S_1-2S_2}{4}\right)\nu D\pi^2+\left(\frac{1+S_1-2S_2}{8}\right)D(1-\nu)\pi^2\right]\bar{\Psi}_x$$
$$+\left[\frac{S_3}{4}Ghab+\left(\frac{1+S_1-2S_2}{4}\right)D\frac{\pi^2 a}{b}+\left(\frac{1+S_1-2S_2}{8}\right)D(1-\nu)\frac{\pi^2 b}{a}\right]\bar{\Psi}_y-\left[\frac{S_3}{4}Gh\pi a+\left(\frac{S_1-S_2}{4}\right)D\frac{\pi^3 a}{b^2}\right. \quad (40)$$
$$\left.+\left(\frac{S_1-S_2}{4}\right)\nu D\frac{\pi^3}{a}+\left(\frac{S_1-S_2}{4}\right)D(1-\nu)\frac{\pi^3}{a}\right]\bar{W}=0,$$

In which

$$P_1(t)=\cos^2\left(\pi\frac{a_0}{a}\cos(\omega t)\right)\cos^2\left(\pi\frac{b_0}{b}\sin(\omega t)\right),$$
$$P_2(t)=\cos\left(\pi\frac{a_0}{a}\cos(\omega t)\right)\sin\left(\pi\frac{a_0}{a}\cos(\omega t)\right)\cos^2\left(\pi\frac{b_0}{b}\sin(\omega t)\right),$$
$$P_3(t)=\cos^2\left(\pi\frac{a_0}{a}\cos(\omega t)\right)\cos\left(\pi\frac{b_0}{b}\sin(\omega t)\right)\sin\left(\pi\frac{b_0}{b}\sin(\omega t)\right), \quad (41)$$
$$P_4(t)=\sin\left(\pi\frac{a_0}{a}\cos(\omega t)\right)\sin\left(\pi\frac{b_0}{b}\sin(\omega t)\right),$$
$$P_5(t)=\cos\left(\pi\frac{a_0}{a}\cos(\omega t)\right)\cos\left(\pi\frac{b_0}{b}\sin(\omega t)\right).$$

In order to nondimensionalize the equations, the dimensionless parameters are defined as follows:

$$\alpha\triangleq\frac{M}{\rho hab},\quad \Omega\triangleq\frac{\omega a^2b^2}{\pi^2\left(a^2+b^2\right)}\sqrt{\frac{\rho h}{D}},\quad \lambda\triangleq\frac{1}{\pi}\sqrt{\frac{\kappa G}{E}},\quad \tau\triangleq\omega t,$$
$$\zeta\triangleq\frac{a_0}{a},\quad \eta\triangleq\frac{b_0}{b},\quad a_r\triangleq\frac{a}{b},\quad r_a\triangleq\frac{h}{a},\quad r_b\triangleq\frac{h}{b},\quad \mathrm{W}\triangleq\frac{\bar{W}}{\sqrt{ab}}, \quad (42)$$
$$\Psi_x\triangleq\bar{\Psi}_x,\quad \Psi_y\triangleq\bar{\Psi}_y,\quad k_w^*\triangleq\frac{k_w a^4b^4}{\pi^4 D\left(a^2+b^2\right)^2},\quad g^*\triangleq\frac{g\rho ha^4b^4}{\pi^4 D\sqrt{ab}\left(a^2+b^2\right)^2}.$$

Finally, the dimensionless coupled ordinary differential equations governing the rectangular plate subjected to an orbiting mass based on the higher-order shear deformation theories are achieved as the following:

$$\Omega^2\left[1+\frac{S_1}{12}\pi^2\left(r_a^2+r_b^2\right)+4\alpha P_1(\tau)\right]\mathrm{W}''+\Omega^2\left[8\alpha\pi\zeta\sin(\tau)P_2(\tau)-8\alpha\pi\eta\cos(\tau)P_3(\tau)\right]\mathrm{W}'$$
$$+\left[S_3\lambda^2\frac{12\left(1-\nu^2\right)}{r_a^2\left(1+a_r^2\right)}+S_1+k_w^*-4\alpha\Omega^2\left(\pi^2\zeta^2\sin^2(\tau)P_1(\tau)+\pi^2\eta^2\cos^2(\tau)P_1(\tau)\right.\right.$$
$$\left.\left.+2\pi^2\zeta\eta\sin(\tau)\cos(\tau)P_4(\tau)P_5(\tau)-\pi\zeta\cos(\tau)P_2(\tau)-\pi\eta\sin(\tau)P_3(\tau)\right)\right]\mathrm{W}$$
$$+\left(\frac{S_1-S_2}{12}\right)\Omega^2\pi\sqrt{r_a^3r_b}\,\Psi_x''-\left[S_3\lambda^2\frac{12\left(1-\nu^2\right)}{\pi\left(r_a\sqrt[4]{\frac{1}{a_r}}+r_b\sqrt[4]{a_r^3}\right)^2}+\frac{(S_1-S_2)}{\pi\left(\sqrt{\frac{1}{a_r}}+\sqrt{a_r^3}\right)}\right]\Psi_x \tag{43}$$
$$+\left(\frac{S_1-S_2}{12}\right)\Omega^2\pi\sqrt{r_a\,r_b^3}\,\Psi_y''-\left[S_3\lambda^2\frac{12\left(1-\nu^2\right)}{\pi\left(r_a\sqrt[4]{\frac{1}{a_r^3}}+r_b\sqrt[4]{a_r}\right)^2}+\frac{(S_1-S_2)}{\pi\left(\sqrt{\frac{1}{a_r^3}}+\sqrt{a_r}\right)}\right]\Psi_y=4\alpha\,g^*P_5(\tau),$$

$$(S_1-S_2)\Omega^2\pi\sqrt{\frac{1}{a_r}}\,\mathrm{W}''+(1+S_1-2S_2)\Omega^2\,\Psi_x''+\left[S_3\lambda^2\frac{144\left(1-\nu^2\right)}{\pi^2\left(r_a^2+r_b^2\right)^2}+(1+S_1-2S_2)\frac{6\left(2+(1-\nu)a_r^2\right)}{\pi^2\left(r_a+a_rr_b\right)^2}\right]\Psi_x$$
$$+(1+S_1-2S_2)\frac{6a_r(1+\nu)}{\pi^2\left(r_a+a_rr_b\right)^2}\Psi_y-\left[S_3\lambda^2\frac{144\left(1-\nu^2\right)}{\pi\sqrt{a_r}\left(r_a^2+r_b^2\right)^2}+(S_1-S_2)\frac{12}{\pi\sqrt{a_r}\left(r_a^2+r_b^2\right)}\right]\mathrm{W}=0, \tag{44}$$

$$(S_1-S_2)\Omega^2\pi\sqrt{a_r}\,\mathrm{W}''+(1+S_1-2S_2)\Omega^2\,\Psi_y''+(1+S_1-2S_2)\frac{6a_r(1+\nu)}{\pi^2\left(r_a+a_rr_b\right)^2}\Psi_x$$
$$+\left[S_3\lambda^2\frac{144\left(1-\nu^2\right)}{\pi^2\left(r_a^2+r_b^2\right)^2}+(1+S_1-2S_2)\frac{6\left(2a_r^2+(1-\nu)\right)}{\pi^2\left(r_a+a_rr_b\right)^2}\right]\Psi_y \tag{45}$$
$$-\left[S_3\lambda^2\frac{144\sqrt{a_r}\left(1-\nu^2\right)}{\pi\left(r_a^2+r_b^2\right)^2}+(S_1-S_2)\frac{12\sqrt{a_r}}{\pi\left(r_a^2+r_b^2\right)}\right]\mathrm{W}=0,$$

In which

$$P_1(\tau)=\cos^2\left(\pi\zeta\cos(\tau)\right)\cos^2\left(\pi\eta\sin(\tau)\right),$$
$$P_2(\tau)=\cos\left(\pi\zeta\cos(\tau)\right)\sin\left(\pi\zeta\cos(\tau)\right)\cos^2\left(\pi\eta\sin(\tau)\right),$$
$$P_3(\tau)=\cos^2\left(\pi\zeta\cos(\tau)\right)\cos\left(\pi\eta\sin(\tau)\right)\sin\left(\pi\eta\sin(\tau)\right), \tag{46}$$
$$P_4(\tau)=\sin\left(\pi\zeta\cos(\tau)\right)\sin\left(\pi\eta\sin(\tau)\right),$$
$$P_5(t)=\cos\left(\pi\zeta\cos(\tau)\right)\cos\left(\pi\eta\sin(\tau)\right).$$

In recent equations, the prime superscript indicates derivative with respect to the dimensionless time τ.

4 ENERGY-RATE METHOD

The energy-rate method is a numerical method for analyzing linear and nonlinear parametrically excited systems. This method, which was first introduced by Nakhaie Jazar [33], can be used to analyze parametric systems and is based on calculating the integral of system energy in one period numerically This method has plenty of advantages in comparison to perturbation methods where the validation of the results is highly dependent on the smallness of the perturbation parameter. In addition, depending on the accuracy of the employed numerical integration method, the energy-rate method can find the value of parameters for a periodic response more accurate than classical methods, no matter if the periodic response is on the boundary of stable and unstable zones or it is a periodic response within the stable or unstable region.The energy-rate method can be applied to any type of time-varying second-order ordinary differential equations in the form of:

$$\ddot{x} + f\left(x\right) + g\left(\ddot{x},\dot{x},x,t\right) = 0, \tag{47}$$

where $f\left(x\right)$ is a single variable function and $g\left(\ddot{x},\dot{x},x,t\right)$ is a time-varying function with the following conditions:

$$g\left(0,0,0,t\right) = 0, \tag{48}$$

$$g\left(\ddot{x},\dot{x},x,t+T\right) = g\left(\ddot{x},\dot{x},x,t\right). \tag{49}$$

In addition, the functions *f* and *g* can depend on finite sets of parameters. Expression (47) may be assumed to be a model of a single mass attached to a spring which is under the non-conservative force of $-g\left(\ddot{x},\dot{x},x,t\right)$. By introducing the kinetic, potential and mechanical energies as $T\left(\dot{x}\right) = \dot{x}^2/2$, $V\left(x\right) = \int f\left(x\right)dx$ and $E = T\left(\dot{x}\right) + V\left(x\right)$, respectively, the time derivative of the energy function can be written as follows:

$$\dot{E} = \frac{d}{dt}\left(E\right) = \frac{d}{dt}\left(\frac{1}{2}\dot{x}^2 + \int\left(f\left(x\right)\dot{x}\right)dt\right) = -\dot{x}\,.g\left(\ddot{x},\dot{x},x,t\right). \tag{50}$$

Next, to examine the stability of the system, the average energy expression during one period cycle is defined as:

$$E_{\text{av}} = \frac{1}{T}\int_0^T \dot{E}\,dt = \frac{1}{T}\int_T^0 \dot{x}\,.g\left(\ddot{x},\dot{x},x,t\right)dt. \tag{51}$$

Now, if E_{av} is greater than zero for some system parameters, the energy will be entered to the system and therefore these parameters are in the unstable region. Otherwise, if E_{av} is less than zero, the system parameters belong to the stable region and consequently the system energy would be reduced accordingly. Moreover, E_{av} will be zero on the boundary separating stable and unstable regions and in this case the associated system parameters belong to a transition curve.

4.1 Applying the energy-rate method to the plate-moving mass system

In this section, by applying the energy-rate method to the equations of the plate-moving mass system, the stable and unstable regions are determined in the moving mass parameters plane ($\alpha - \Omega$ plane). For this end, neglecting the gravity effect, the coupled Eqs. (43-45) are introduced in the vector-matrix form as the following:

$$\Omega^2\left(M_1+4\alpha M_2(\tau)\right)\mathbf{Q}''+8\alpha\Omega^2 C_1(\tau)\mathbf{Q}'+\left(K_1-4\alpha\Omega^2 K_2(\tau)\right)\mathbf{Q}=0, \tag{52}$$

where the elements of vectors and matrices are presented in Appendix B. By rewriting Eq. (52) in the form of Eq. (47) we have:

$$\mathbf{Q}''+f(\mathbf{Q})+g\left(\mathbf{Q}'',\mathbf{Q}',\mathbf{Q},\tau\right)=0, \tag{53}$$

In which:

$$\begin{aligned} f(\mathbf{Q})&=\frac{1}{\Omega^2}M_1^{-1}K_1\mathbf{Q},\\ g\left(\mathbf{Q}'',\mathbf{Q}',\mathbf{Q},\tau\right)&=4\alpha M_1^{-1}M_2(\tau)\,\mathbf{Q}''+8\alpha M_1^{-1}C_1(\tau)\,\mathbf{Q}'-4\alpha M_1^{-1}K_2(\tau)\mathbf{Q}. \end{aligned} \tag{54}$$

The average energy during a period is obtained as:

$$E_{av}=\frac{1}{2\pi}\int_0^{2\pi}\dot{E}\,dt=\frac{1}{2\pi}\int_{2\pi}^{0}\mathbf{Q}'^{T}.g\left(\mathbf{Q}'',\mathbf{Q}',\mathbf{Q},\tau\right)dt. \tag{55}$$

In order to identify those parameters of the moving mass which belong to boundary curves and separate the stable and unstable regions, an algorithm has been written in a computer software which by meshing the problem parameters plane, solves the governing coupled ODEs for each pair of (α,Ω) numerically, and calculates the value of E_{av} and extracts the stability boundary curves (everywhere $|E_{\text{av}}|\ll 1$).

5 RESULTS AND DISCUSSIONS

In this section, the dynamic stability of the system is examined based on the higher-order shear deformation theories. Effects of the plate thickness ratio, the radii of moving mass movement path and the elastic foundation stiffness on the parametric regions are evaluated. In the figures provided in the following, the regions surrounded by two curves intersecting on the Ω axis depict the unstable zones. These unstable regions identified in the moving mass parameters plane are completely relevant to the occurrence of principle parametric resonance in the mentioned system. Indeed, the condition for parametric resonance is provided when the forcing frequency is almost close to twice of the natural frequency of the unforced system.

Fig. 3 shows the unstable region of $\alpha-\Omega$ plane based on different higher order theories including TSDT, ITSDT, SSDT, HSDT and ESDT. The dimensionless parameters in these analyses are set to be as $a_r=1$, $r_a=r_b=0.2$, $\zeta=0.15$, $\eta=0.3$, $\nu=0.3$ and $k_w^*=0$. As it can be seen, the ITSDT predicts the unstable region at lower frequencies compared to other theories. This is because of the fact that the ITSDT theory considers the system softer by setting the parameter S_2 equal to zero. On the other hand, the ESDT approximates the parametric resonance frequencies higher than those approximated by other theories. However, there is no appreciable difference between the results of TSDT, SSDT and ESDT. In addition, it can be understood from Fig. 3 that by increasing the mass of the traveling load, the plates will become unstable for a wider range of the mass rotation frequencies. Also, from the figure it can be concluded that the critical rotation frequencies are lower for heavier masses. In the rest of the paper in order to investigate the effects of different parameters on the system stability, just the results of TSDT theory are considered.

Fig. 4 shows the unstable region of the system for different values of the plate thickness ratio, r_a. The dimensionless parameters in these analyses are as $a_r=1$, $\zeta=0.15$, $\eta=0.3$, $\nu=0.3$ and $k_w^*=0$. It is worth to mention that when the ratio of the plate thickness to one of its dimensions is less than or equal to 0.02 $(r_a\le 0.02)$, the

plate would be considered as a thin structure [32], [34-36] and so the results of the shear deformation theory will become identical to those of the classic plate theory. It is observed from Fig. 4 that increasing the plate thickness ratio shifts the unstable region downwards (i.e. lower resonance frequencies), which means that the Kirchhoff's theory overestimates the critical frequencies, especially for thick plates. The reason is that the shear deformation theories predict the resonance frequencies of thick plates more accurately by considering their higher degrees of freedom.

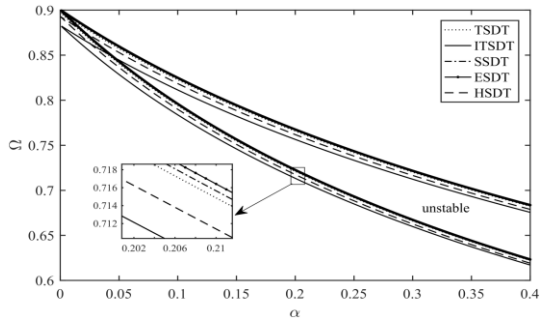

Fig.3
Stability diagram for the plate-mass system based on various higher-order shear deformation theories.

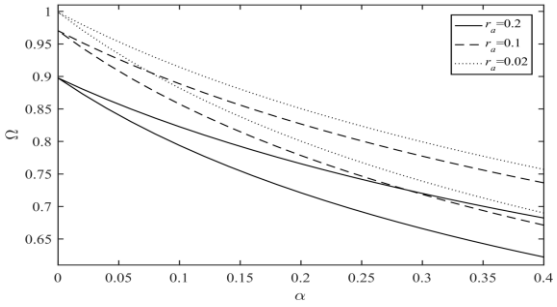

Fig.4
Effect of the plate thickness ratio on the unstable region.

The effect of dimensionless semi-minor and semi-major axes parameters of the elliptical path, (ζ,η), on the system stability has been investigated by considering other parameters as $a_r = 1$, $r_a = r_b = 0.2$, $\nu = 0.3$ and $k_w^* = 0$. As shown in Fig. 5, for a specific value of the travelling load mass α, the plate vibrations will become unstable for a wider range of the dimensionless frequency Ω when the radii of the path are increased. Besides, it can be seen that if α tends to zero, the difference between the results of diverse radii will be reduced. This implies that for the case of moving force (neglecting inertial terms of the moving object), different values of the radii of the motion path lead to identical critical rotation frequency.

The effect of Winkler foundation on the unstable region is illustrated in Fig. 6. As it reveals, an increase in the elastic foundation stiffness leads to an increase in the parametric resonance frequency of the system. In other words, in the presence of an elastic foundation with a suitable stiffness, the origin of the unstable region switches to higher frequencies of the orbiting mass and consequently occurrence of parametric resonance is postponed. This is because of the fact that an escalation in the foundation stiffness increases the stiffness of the whole structure. So, selecting appropriate elastic foundation may lead to a change in the natural frequencies of the system and consequently a feasibility to avoid resonance and instability.

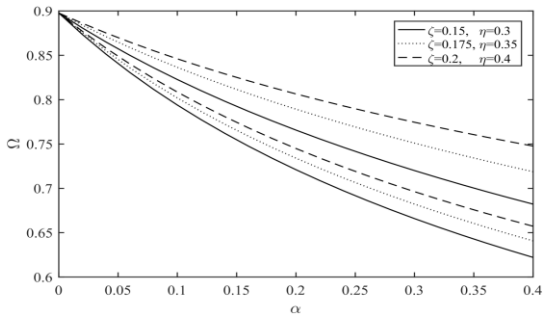

Fig.5
Effect of the movement path radii on the unstable region.

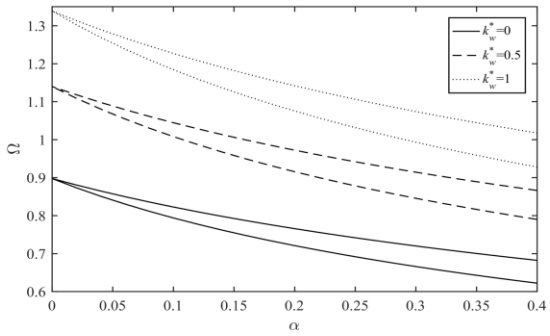

Fig.6
Effect of the Winkler foundation stiffness on the unstable region.

6 VERIFICATION

As mentioned earlier, when the plate thickness ratio is less than or equal to 0.02, the results obtained from shear deformation theories and the Kirchhoff's plate theory should be matched. According to this, in order to verify the utilized method in this paper, the obtained results are compared with those reported by Pirmoradian et al. [25], where a circular path has been considered for the mass motion and the plate has been modeled based on the Kirchhoff's plate theory by considering plate of low thickness. For this purpose, by taking $a_0 = b_0$ and so changing the elliptical path to the special case of circular path, and also setting the system parameters as $a_r = 2$, $r_a = 0.01$, $r_b = 0.02$, $\zeta = 0.15$, $\eta = 0.3$, $\nu = 0.3$ and $k_w^* = 0$ the comparison is possible. As depicted in Fig. 7, the good agreement between the results proves the accuracy of the results obtained by the energy-rate method.

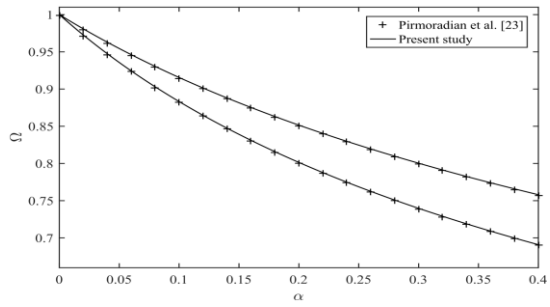

Fig.7
Unstable region of the parameters plane.

7 CONCLUSIONS

Different higher-order shear deformation theories including third-order shear deformation theory, improved third-order shear deformation theory, sinusoidal shear deformation theory, exponential shear deformation theory and hyperbolic shear deformation theory were developed to study the dynamic stability of a simply supported plate carrying a mass moving on an elliptical path. The differential equations of motion were obtained using the Hamilton's principle and were solved utilizing the Galerkin method along with trigonometric shape functions. The stable and unstable regions of the system parameters plane were calculated using the energy-rate method, and the effects of different parameters such as the plate thickness ratio, the movement path radii and the stiffness of the Winkler foundation on the system stability were studied. The results reveal that for orbiting motion of the mass on the plate, there is a region of instability in the parameters plane which cannot be ignored in design of related applications. This unstable region emerges at lower frequencies of the orbiting mass for the ITSDT in comparison with other theories. However, the difference between the results of TSDT, SSDT and ESDT are not substantial. Also, the stability diagrams highlight the great influence of the mass of the traveling load on the instability conditions, so that its increase leads to lower critical frequencies of motion of the orbiting mass. The results show that an increase in the movement path radii increases the area of unstable region. Moreover, escalation the Winkler foundation stiffness enhances the stability of the system.

APPENDIX A

The Components of matrices and vectors expressed in Eqs. (33), (34) and (35):

$$
\begin{aligned}
M_{ij} &= \rho h \int_A \tilde{w}_i(x,y)\tilde{w}_j(x,y)dA - S_1\rho J\left(\int_A \frac{\partial^2 \tilde{w}_i(x,y)}{\partial x^2}\tilde{w}_j(x,y)dA + \int_A \frac{\partial^2 \tilde{w}_i(x,y)}{\partial y^2}\tilde{w}_j(x,y)dA\right)\\
&\quad + M\,\tilde{w}_i\left(x_M(t),y_M(t)\right)\tilde{w}_j\left(x_M(t),y_M(t)\right),\\
C_{ij} &= 2M\,\dot{x}\,\frac{\partial \tilde{w}_i\left(x_M(t),y_M(t)\right)}{\partial x}\tilde{w}_j\left(x_M(t),y_M(t)\right) + 2M\,\dot{y}\,\frac{\partial \tilde{w}_i\left(x_M(t),y_M(t)\right)}{\partial y}\tilde{w}_j\left(x_M(t),y_M(t)\right),\\
K_{ij} &= -S_3 Gh\left(\int_A \frac{\partial^2 \tilde{w}_i(x,y)}{\partial x^2}\tilde{w}_j(x,y)dA + \int_A \frac{\partial^2 \tilde{w}_i(x,y)}{\partial y^2}\tilde{w}_j(x,y)dA\right)\\
&\quad - S_1\left(\int_A \frac{\partial^4 \tilde{w}_i(x,y)}{\partial x^4}\tilde{w}_j(x,y)dA + \nu\int_A \frac{\partial^4 \tilde{w}_i(x,y)}{\partial x^2\partial y^2}\tilde{w}_j(x,y)dA\right)\\
&\quad - S_1\left(\int_A \frac{\partial^4 \tilde{w}_i(x,y)}{\partial y^4}\tilde{w}_j(x,y)dA + \nu\int_A \frac{\partial^4 \tilde{w}_i(x,y)}{\partial x^2\partial y^2}\tilde{w}_j(x,y)dA\right)\\
&\quad + \frac{D(1-\nu)}{2}\left(4S_1\int_A \frac{\partial^4 \tilde{w}_i(x,y)}{\partial x^2\partial y^2}\tilde{w}_j(x,y)dA\right) + \int_A k_w\tilde{w}_i(x,y)\tilde{w}_j(x,y)dA\\
&\quad + M\,\dot{x}^2\,\frac{\partial^2 \tilde{w}_i\left(x_M(t),y_M(t)\right)}{\partial x^2}\tilde{w}_j\left(x_M(t),y_M(t)\right) + M\,\dot{y}^2\,\frac{\partial^2 \tilde{w}_i\left(x_M(t),y_M(t)\right)}{\partial y^2}\tilde{w}_j\left(x_M(t),y_M(t)\right)\\
&\quad + 2M\,\dot{x}\dot{y}\,\frac{\partial^2 \tilde{w}_i\left(x_M(t),y_M(t)\right)}{\partial x\,\partial y}\tilde{w}_j\left(x_M(t),y_M(t)\right) + M\,\ddot{x}\,\frac{\partial \tilde{w}_i\left(x_M(t),y_M(t)\right)}{\partial x}\tilde{w}_j\left(x_M(t),y_M(t)\right)\\
&\quad + M\,\ddot{y}\,\frac{\partial \tilde{w}_i\left(x_M(t),y_M(t)\right)}{\partial y}\tilde{w}_j\left(x_M(t),y_M(t)\right),\\
D_{ij} &= -(S_1-S_2)\rho J\left(\int_A \frac{\partial \tilde{\psi}_{xi}(x,y)}{\partial x}\tilde{w}_j(x,y)dA\right),\\
R_{ij} &= S_3 Gh\left(\int_A \frac{\partial \tilde{\psi}_{xi}(x,y)}{\partial x}\tilde{w}_j(x,y)dA\right) - D(S_1-S_2)\left(\int_A \frac{\partial^3 \tilde{\psi}_{xi}(x,y)}{\partial x^3}\tilde{w}_j(x,y)dA\right)\\
&\quad - D(S_1-S_2)\left(\nu\int_A \frac{\partial^3 \tilde{\psi}_{xi}(x,y)}{\partial x\,\partial y^2}\tilde{w}_j(x,y)dA\right) - \frac{D(1-\nu)}{2}\left(2(S_1-S_2)\int_A \frac{\partial^3 \tilde{\psi}_{xi}(x,y)}{\partial x\,\partial y^2}\tilde{w}_j(x,y)dA\right),\\
B_{ij} &= -(S_1-S_2)\rho J\left(\int_A \frac{\partial \tilde{\psi}_{yi}(x,y)}{\partial y}\tilde{w}_j(x,y)dA\right),\\
T_{ij} &= S_3 Gh\left(\int_A \frac{\partial \tilde{\psi}_{yi}(x,y)}{\partial y}\tilde{w}_j(x,y)dA\right) - D(S_1-S_2)\left(\nu\int_A \frac{\partial^3 \tilde{\psi}_{yi}(x,y)}{\partial x^2\partial y}\tilde{w}_j(x,y)dA\right)\\
&\quad - D(S_1-S_2)\left(\int_A \frac{\partial^3 \tilde{\psi}_{yi}(x,y)}{\partial y^3}\tilde{w}_j(x,y)dA\right) - \frac{D(1-\nu)}{2}\left(2(S_1-S_2)\int_A \frac{\partial^3 \tilde{\psi}_{yi}(x,y)}{\partial x^2\partial y}\tilde{w}_j(x,y)dA\right),\\
F_j &= mg\,\tilde{w}_j\left(x_m(t),y_m(t)\right),
\end{aligned}
$$

$$\bar{M}_{ij} = \left(S_1 - S_2\right)\left(\rho J \int_A \frac{\partial \tilde{w}_i\left(x,y\right)}{\partial x} \tilde{\psi}_{xj}\left(x,y\right) dA \right),$$

$$\bar{D}_{ij} = \left(1 + S_1 - 2S_2\right)\left(\rho J \int_A \tilde{\psi}_{xi}\left(x,y\right) \tilde{\psi}_{xj}\left(x,y\right) dA \right),$$

$$\bar{R}_{ij} = -\left(1 + S_1 - 2S_2\right)\left(\int_A \frac{\partial^2 \tilde{\psi}_{xi}\left(x,y\right)}{\partial x^2} \tilde{\psi}_{xj}\left(x,y\right) dA \right)$$

$$-\frac{D\left(1-\nu\right)}{2}\left(\left(1 + S_1 - 2S_2\right) \int_A \frac{\partial^2 \tilde{\psi}_{xi}\left(x,y\right)}{\partial y^2} \tilde{\psi}_{xj}\left(x,y\right) dA \right) + S_3 Gh \left(\int_A \tilde{\psi}_{xi}\left(x,y\right) \tilde{\psi}_{xj}\left(x,y\right) dA \right),$$

$$\bar{K}_{ij} = \left(S_1 - S_2\right)\left(\int_A \frac{\partial^3 \tilde{w}_i\left(x,y\right)}{\partial x^3} \tilde{\psi}_{xj}\left(x,y\right) dA + \nu \int_A \frac{\partial^3 \tilde{w}_i\left(x,y\right)}{\partial x\, \partial y^2} \tilde{\psi}_{xj}\left(x,y\right) dA \right)$$

$$+ 2\left(S_1 - S_2\right)\left(\int_A \frac{\partial^3 \tilde{w}_i\left(x,y\right)}{\partial x\, \partial y^2} \tilde{\psi}_{xj}\left(x,y\right) dA \right) - S_3 Gh \left(\int_A \frac{\partial \tilde{w}_i\left(x,y\right)}{\partial x} \tilde{\psi}_{xj}\left(x,y\right) dA \right),$$

$$\bar{T}_{ij} = -D\left(1 + S_1 - 2S_2\right)\left(\nu \int_A \frac{\partial^2 \tilde{\psi}_{yi}\left(x,y\right)}{\partial x\, \partial y} \tilde{\psi}_{xj}\left(x,y\right) dA \right) - \frac{D\left(1-\nu\right)}{2}\left(1 + S_1 - 2S_2\right)\left(\int_A \frac{\partial^2 \tilde{\psi}_{yi}\left(x,y\right)}{\partial x\, \partial y} \tilde{\psi}_{xj}\left(x,y\right) dA \right),$$

$$\tilde{M}_{ij} = \left(S_1 - S_2\right)\left(\rho J \int_A \frac{\partial \tilde{w}_i\left(x,y\right)}{\partial y} \tilde{\psi}_{yj}\left(x,y\right) dA \right),$$

$$\tilde{B}_{ij} = \left(1 + S_1 - 2S_2\right)\left(\rho J \int_A \tilde{\psi}_{yi}\left(x,y\right) \tilde{\psi}_{yj}\left(x,y\right) dA \right),$$

$$\tilde{R}_{ij} = -D\left(1 + S_1 - 2S_2\right)\left(\nu \int_A \frac{\partial^2 \tilde{\psi}_{xi}\left(x,y\right)}{\partial x\, \partial y} \tilde{\psi}_{yj}\left(x,y\right) dA \right) - \frac{D\left(1-\nu\right)}{2}\left(1 + S_1 - 2S_2\right)\left(\int_A \frac{\partial^2 \tilde{\psi}_{xi}\left(x,y\right)}{\partial x\, \partial y} \tilde{\psi}_{yj}\left(x,y\right) dA \right),$$

$$\tilde{K}_{ij} = \left(S_1 - S_2\right)\left(\int_A \frac{\partial^3 \tilde{w}_i\left(x,y\right)}{\partial y^3} \tilde{\psi}_{yj}\left(x,y\right) dA + \nu \int_A \frac{\partial^3 \tilde{w}_i\left(x,y\right)}{\partial x^2 \partial y} \tilde{\psi}_{yj}\left(x,y\right) dA \right)$$

$$+ 2\left(S_1 - S_2\right)\left(\int_A \frac{\partial^3 \tilde{w}_i\left(x,y\right)}{\partial x^2 \partial y} \tilde{\psi}_{yj}\left(x,y\right) dA \right) - S_3 Gh \left(\int_A \frac{\partial \tilde{w}_i\left(x,y\right)}{\partial y} \tilde{\psi}_{yj}\left(x,y\right) dA \right),$$

$$\tilde{T}_{ij} = -D\left(1 + S_1 - 2S_2\right)\left(\int_A \frac{\partial^2 \tilde{\psi}_{yi}\left(x,y\right)}{\partial y^2} \tilde{\psi}_{yj}\left(x,y\right) dA \right) - \frac{D\left(1-\nu\right)}{2}\left(1 + S_1 - 2S_2\right)\left(\int_A \frac{\partial^2 \tilde{\psi}_{yi}\left(x,y\right)}{\partial x^2} \tilde{\psi}_{yj}\left(x,y\right) dA \right)$$

$$+ S_3 Gh \left(\int_A \tilde{\psi}_{yi}\left(x,y\right) \tilde{\psi}_{yj}\left(x,y\right) dA \right),$$

$$\bar{W} = \left[\bar{W}_1\left(t\right), \bar{W}_2\left(t\right), \ldots, \bar{W}_n\left(t\right)\right]^T, \qquad \bar{\Psi}_x = \left[\bar{\Psi}_{x1}\left(t\right), \bar{\Psi}_{x2}\left(t\right), \ldots, \bar{\Psi}_{xn}\left(t\right)\right]^T, \qquad \bar{\Psi}_y = \left[\bar{\Psi}_{y1}\left(t\right), \bar{\Psi}_{y2}\left(t\right), \ldots, \bar{\Psi}_{yn}\left(t\right)\right]^T.$$

APPENDIX B

The components of matrices and vectors of Eq. (52):

$$M_1=\begin{bmatrix} 1+\frac{S_1}{12}\pi^2\left(r_a^2+r_b^2\right) & \left(\frac{S_1-S_2}{12}\right)\pi\sqrt{r_a^3 r_b} & \left(\frac{S_1-S_2}{12}\right)\pi\sqrt{r_a\, r_b^3} \\ \left(S_1-S_2\right)\pi\sqrt{\frac{1}{a_r}} & \left(1+S_1-2S_2\right) & 0 \\ \left(S_1-S_2\right)\pi\sqrt{a_r} & 0 & \left(1+S_1-2S_2\right) \end{bmatrix},$$

$$M_2(\tau)=\begin{bmatrix} P_1(\tau) & 0 & 0 \\ 0 & 0 & 0 \\ 0 & 0 & 0 \end{bmatrix}, \quad C_1(\tau)=\begin{bmatrix} \pi\zeta\sin(\tau)P_2(\tau)-\pi\eta\cos(\tau)P_3(\tau) & 0 & 0 \\ 0 & 0 & 0 \\ 0 & 0 & 0 \end{bmatrix},$$

$$K_1=\begin{bmatrix} k_{11} & k_{12} & k_{13} \\ k_{21} & k_{22} & k_{23} \\ k_{31} & k_{32} & k_{33} \end{bmatrix}, \quad K_2(\tau)=\begin{bmatrix} \bar{k}_{11} & 0 & 0 \\ 0 & 0 & 0 \\ 0 & 0 & 0 \end{bmatrix}, \quad Q^*=\left[\mathrm{W}^*,\Psi_x^*,\Psi_y^*\right]^T,$$

$$k_{11}=S_3\lambda^2\frac{12\left(1-\nu^2\right)}{r_a^2\left(1+a_r^2\right)}+S_1+k_w^*, \qquad k_{12}=-S_3\lambda^2\frac{12\left(1-\nu^2\right)}{\pi\left(r_a\sqrt[4]{\frac{1}{a_r}}+r_b\sqrt[4]{a_r^3}\right)^2}-\frac{\left(S_1-S_2\right)}{\pi\left(\sqrt{\frac{1}{a_r}}+\sqrt{a_r^3}\right)},$$

$$k_{13}=-S_3\lambda^2\frac{12\left(1-\nu^2\right)}{\pi\left(r_a\sqrt[4]{\frac{1}{a_r^3}}+r_b\sqrt[4]{a_r}\right)^2}-\frac{\left(S_1-S_2\right)}{\pi\left(\sqrt{\frac{1}{a_r^3}}+\sqrt{a_r}\right)},$$

$$k_{21}=-S_3\lambda^2\frac{144\left(1-\nu^2\right)}{\pi\sqrt{a_r}\left(r_a^2+r_b^2\right)^2}-\left(S_1-S_2\right)\frac{12}{\pi\sqrt{a_r}\left(r_a^2+r_b^2\right)},$$

$$k_{22}=S_3\lambda^2\frac{144\left(1-\nu^2\right)}{\pi^2\left(r_a^2+r_b^2\right)^2}+\left(1+S_1-2S_2\right)\frac{6\left(2+(1-\nu)a_r^2\right)}{\pi^2\left(r_a+a_r r_b\right)^2},$$

$$k_{23}=\left(1+S_1-2S_2\right)\frac{6a_r\left(1+\nu\right)}{\pi^2\left(r_a+a_r r_b\right)^2}, \qquad k_{31}=-S_3\lambda^2\frac{144\sqrt{a_r}\left(1-\nu^2\right)}{\pi\left(r_a^2+r_b^2\right)^2}-\left(S_1-S_2\right)\frac{12\sqrt{a_r}}{\pi\left(r_a^2+r_b^2\right)},$$

$$k_{32}=\left(1+S_1-2S_2\right)\frac{6a_r\left(1+\nu\right)}{\pi^2\left(r_a+a_r r_b\right)^2}, \qquad k_{33}=S_3\lambda^2\frac{144\left(1-\nu^2\right)}{\pi^2\left(r_a^2+r_b^2\right)^2}+\left(1+S_1-2S_2\right)\frac{6\left(2a_r^2+(1-\nu)\right)}{\pi^2\left(r_a+a_r r_b\right)^2},$$

$$\bar{k}_{11}=\pi^2\zeta^2\sin^2(\tau)P_1(\tau)+\pi^2\eta^2\cos^2(\tau)P_1(\tau)+2\pi^2\zeta\eta\sin(\tau)\cos(\tau)P_4(\tau)P_5(\tau)$$
$$-\pi\zeta\cos(\tau)P_2(\tau)-\pi\eta\sin(\tau)P_3(\tau).$$

REFERENCES

[1] Karimi A.H., Ziaei-Rad S., 2015, Nonlinear coupled longitudinal–transverse vibration analysis of a beam subjected to a moving mass traveling with variable speed, *Archive of Applied Mechanics* **85**: 1941-1960.

[2] Lv J., Kang H., 2018, Nonlinear dynamic analysis of cable-stayed arches under primary resonance of cables, *Archive of Applied Mechanics* **88**: 1-14.

[3] Babagi P.N., Neya B.N., Dehestani M., 2017, Three dimensional solution of thick rectangular simply supported plates under a moving load, *Meccanica* **52**: 3675-3692.

[4] Ozgan K., Daloglu A.T., Karakaş Aİ., 2013, A parametric study for thick plates resting on elastic foundation with variable soil depth, *Archive of Applied Mechanics* **83**: 549-558.

[5] Rofooei F.R., Enshaeian A., Nikkhoo A., 2017, Dynamic response of geometrically nonlinear, elastic rectangular plates under a moving mass loading by inclusion of all inertial components, *Journal of Sound and Vibration* **394**: 497-514.

[6] Enshaeian A., Rofooei F.R., 2014, Geometrically nonlinear rectangular simply supported plates subjected to a moving mass, *Acta Mechanica* **225**: 595-608.

[7] Wang Y.Q., Zu J.W., 2017, Nonlinear steady-state responses of longitudinally traveling functionally graded material plates in contact with liquid, *Composite Structures* **164**: 130-144.

[8] Wang Y.Q., Zu J.W., 2017, Nonlinear dynamic thermoelastic response of rectangular FGM plates with longitudinal velocity, *Composites Part B: Engineering* **117**: 74-88.

[9] Niaz M., Nikkhoo A., 2015, Inspection of a rectangular plate dynamics under a moving mass with varying velocity utilizing BCOPs, *Latin American Journal of Solids and Structures* **12**: 317-332.

[10] Frýba L., 1999, *Vibration of Solids and Structures under Moving Loads*, Thomas Telford House, London.

[11] Nikkhoo A., Rofooei F.R., 2012, Parametric study of the dynamic response of thin rectangular plates traversed by a moving mass, *Acta Mechanica* **223**: 15-27.

[12] Esen I., 2013, A new finite element for transverse vibration of rectangular thin plates under a moving mass, *Finite Elements in Analysis and Design* **66**: 26-35.

[13] Nikkhoo A., Hassanabadi M.E., Azam S.E., Amiri J.V., 2014, Vibration of a thin rectangular plate subjected to series of moving inertial loads, *Mechanics Research Communications* **55**: 105-113.

[14] Hassanabadi M.E., Attari N.K.A., Nikkhoo A., 2016, Resonance of a rectangular plate influenced by sequential moving masses, *Coupled Systems Mechanics* **5**: 87-100.

[15] Gbadeyan J.A., Dada M.S., 2006, Dynamic response of a Mindlin elastic rectangular plate under a distributed moving mass, *International journal of mechanical sciences* **48**: 323-340.

[16] Amiri J.V., Nikkhoo A., Davoodi M.R., Hassanabadi M.E., 2013, Vibration analysis of a Mindlin elastic plate under a moving mass excitation by eigenfunction expansion method, *Thin-Walled Structures* **62**: 53-64.

[17] Ansari M., Esmailzadeh E., Younesian D., 2010, Internal-external resonance of beams on non-linear viscoelastic foundation traversed by moving load, *Nonlinear Dynamics* **61**: 163-182.

[18] Rao G.V., 2000, Linear dynamics of an elastic beam under moving loads, *Journal of Vibration and Acoustics* **122**: 281-289.

[19] Nelson H.D., Conover R.A., 1971, Dynamic stability of a beam carrying moving masses, *Journal of Applied Mechanics* **38**: 1003-1006.

[20] Pirmoradian M., Keshmiri M., Karimpour H., 2014, Instability and resonance analysis of a beam subjected to moving mass loading via incremental harmonic balance method, *Journal of Vibroengineering* **16**: 2779-2789.

[21] Pirmoradian M., Keshmiri M., Karimpour H., 2015, On the parametric excitation of a Timoshenko beam due to intermittent passage of moving masses: instability and resonance analysis, *Acta Mechanica* **226**: 1241-1253.

[22] Yang T-Z., Fang B., 2012, Stability in parametric resonance of an axially moving beam constituted by fractional order material, *Archive of Applied Mechanics* **82**: 1763-1770.

[23] Torkan E., Pirmoradian M., Hashemian M., 2018, On the parametric and external resonances of rectangular plates on an elastic foundation traversed by sequential masses, *Archive of Applied Mechanics* **88**: 1411-1428.

[24] Torkan E., Pirmoradian M., Hashemian M., 2017, Occurrence of parametric resonance in vibrations of rectangular plates resting on elastic foundation under passage of continuous series of moving masses, *Modares Mechanical Engineering* **17**: 225-236.

[25] Pirmoradian M., Torkan E., Karimpour H., 2018, Parametric resonance analysis of rectangular plates subjected to moving inertial loads via IHB method, *International Journal of Mechanical Sciences* **142**: 191-215.

[26] Karimpour H., Pirmoradian M., Keshmiri M., 2016, Instance of hidden instability traps in intermittent transition of moving masses along a flexible beam, *Acta Mechanica* **227**: 1213-1224.

[27] Reddy J.N., 1984, A simple higher-order theory for laminated composite plates, *Journal of Applied Mechanics* **51**: 745-752.

[28] Shi G., 2007, A new simple third-order shear deformation theory of plates, *International Journal of Solids and Structures* **44**: 4399-4417.

[29] Touratier M., 1991, An efficient standard plate theory, *International Journal of Engineering Science* **29**: 901-916.

[30] Karama M., Afaq K.S., Mistou S., 2003, Mechanical behaviour of laminated composite beam by the new multi-layered laminated composite structures model with transverse shear stress continuity, *International Journal of Solids and Structures* **40**: 1525-1546.

[31] El Meiche N., Tounsi A., Ziane N., Mechab I., 2011, A new hyperbolic shear deformation theory for buckling and vibration of functionally graded sandwich plate, *International Journal of Mechanical Sciences* **53**: 237-247.

[32] Torkan E., Pirmoradian M., Hashemian M., 2019, Instability inspection of parametric vibrating rectangular mindlin plates lying on Winkler foundations under periodic loading of moving masses, *Acta Mechanica Sinica* **35**: 242-263.

[33] Jazar G.N., 2004, Stability chart of parametric vibrating systems using energy-rate method, *International Journal of Non-Linear Mechanics* **39**: 1319-1331.

[34] Torkan E., Pirmoradian M., Hashemian M., 2019, Dynamic instability analysis of moderately thick rectangular plates influenced by an orbiting mass based on the first-order shear deformation theory, *Modares Mechanical Engineering* **19**: 2203-2213.

[35] Pirmoradian M., Karimpour H., 2017, Parametric resonance and jump analysis of a beam subjected to periodic mass transition, *Nonlinear Dynamics* **89**: 2141-2154.

[36] Pirmoradian M., Karimpour H., 2017, Nonlinear effects on parametric resonance of a beam subjected to periodic mass transition, *Modares Mechanical Engineering* **17**: 284-292.